AGU PUBLICATIONS

Geophysical Research Letters

RESEARCH LETTER
10.1002/2017GL076397

Key Points:
- The recent decrease in WNP TCs was driven by an intensification of vertical wind shear in the southeastern/eastern WNP
- The intensified vertical wind shear in the southeastern/eastern WNP arose primarily from the enhanced SST warming in the North Atlantic
- The SST anomalies in the tropical Pacific associated with the negative PDO and the anthropogenic forcing play only secondary roles

Supporting Information:
- Supporting Information S1

Correspondence to:
W. Zhang,
wei-zhang-3@uiowa.edu

Citation:
Zhang, W., Vecchi, G. A., Murakami, H., Villarini, G., Delworth, T. L., Yang, X., & Jia, L. (2018). Dominant role of Atlantic Multidecadal Oscillation in the recent decadal changes in western North Pacific tropical cyclone activity. *Geophysical Research Letters*, *45*, 354–362. https://doi.org/10.1002/2017GL076397

Received 14 NOV 2017
Accepted 19 DEC 2017
Accepted article online 27 DEC 2017
Published online 11 JAN 2018

Dominant Role of Atlantic Multidecadal Oscillation in the Recent Decadal Changes in Western North Pacific Tropical Cyclone Activity

Wei Zhang[1], Gabriel A. Vecchi[2,3], Hiroyuki Murakami[4,5], Gabriele Villarini[1], Thomas L. Delworth[4,5], Xiaosong Yang[4], and Liwei Jia[6,7]

[1]IIHR-Hydroscience and Engineering, University of Iowa, Iowa City, IA, USA, [2]Department of Geosciences, Princeton University, Princeton, NJ, USA, [3]Princeton Environmental Institute, Princeton University, Princeton, NJ, USA, [4]National Oceanic and Atmospheric Administration/Geophysical Fluid Dynamics Laboratory, Princeton, NJ, USA, [5]Atmospheric and Oceanic Sciences Program, Princeton University, Princeton, NJ, USA, [6]Climate Prediction Center, NOAA/NWS/NCEP, College Park, MD, USA, [7]Innovim, LLC, Greenbelt, MD, USA

Abstract Over the 1997–2014 period, the mean frequency of western North Pacific (WNP) tropical cyclones (TCs) was markedly lower (~18%) than the period 1980–1996. Here we show that these changes were driven by an intensification of the vertical wind shear in the southeastern/eastern WNP tied to the changes in the Walker circulation, which arose primarily in response to the enhanced sea surface temperature (SST) warming in the North Atlantic, while the SST anomalies associated with the negative phase of the Pacific Decadal Oscillation in the tropical Pacific and the anthropogenic forcing play only secondary roles. These results are based on observations and experiments using the Geophysical Fluid Dynamics Laboratory Forecast-oriented Low-ocean Resolution Coupled Climate Model coupled climate model. The present study suggests a crucial role of the North Atlantic SST in causing decadal changes to WNP TC frequency.

Plain Language Summary The western North Pacific (WNP) is the most active ocean basin for tropical cyclone (TC) activity, with very significant societal and economic impacts. Over 1997–2014, the number of WNP TCs has abruptly decreased (~18%). We examine the relative roles of sea surface temperature (SST) changes and anthropogenic forcing in this decrease of WNP TCs. This change of WNP TCs is driven by an intensification of the vertical wind shear in the southeastern/eastern WNP which is mainly tied to SST warming in the North Atlantic, while the SST anomalies associated with the negative Pacific Decadal Oscillation phase and the anthropogenic forcing only play secondary roles. The present study suggests a crucial role of the North Atlantic SST in causing the observed decadal change in WNP TC frequency.

1. Introduction

The frequency, intensity, and tracks of tropical cyclones (TCs) can be influenced by both natural climate variability (Chan, 2008; Kossin et al., 2016; Wang & Chan, 2002) and anthropogenic forcing (Knutson et al., 2010; Murakami et al., 2012; Villarini et al., 2011). The western North Pacific (WNP) is the most active ocean basin for TC activity, with very significant societal and economic impacts (Emanuel, 2005a; Peduzzi et al., 2012). Since 1993, however, a decreasing trend in WNP TC power dissipation index (PDI, Emanuel, 2005b, 2007) has been identified, with the main culprit being the reduced WNP TC frequency associated with intensified vertical wind shear (Lin & Chan, 2015).

Recently, several studies have reported that the reduced WNP TC activity since the late 1990s may be tied with internal climate modes (e.g., PDO; Mantua et al., 1997), aerosol changes, and global-warming-related upper-troposphere warming (Choi et al., 2015; He et al., 2015; Liu & Chan, 2012; Takahashi et al., 2017; Wu et al., 2015). While different hypotheses have been proposed, there is still no consensus regarding the drivers of this observed decrease. Moreover, the Atlantic sea surface temperature (SST) anomalies (e.g., the Atlantic Multidecadal Oscillation (AMO)) can modulate changes in the Pacific climate (Delworth et al., 2016; England et al., 2014; Kucharski et al., 2016; Li et al., 2015; McGregor et al., 2014; Ruprich-Robert et al., 2017; Sun et al., 2017; Zhang & Delworth, 2007) and WNP TC frequency (Yu et al., 2015; Zhang, Vecchi, Villarini, Murakami, Rosati, et al., 2017). Therefore, despite previous efforts, what caused the observed decadal change in WNP TC frequency since 1980 remains an open question. The PDO and AMO switched their phases in the middle-to-late 1990s, after which the sharp decrease in WNP TC frequency occurred. It is therefore

reasonable to postulate that the observed decadal change in WNP TC frequency may be linked to the observed recent changes in these climate modes. The climate system response to anthropogenic forcing occurs in the presence of substantial natural climate variability, and it is difficult to unambiguously separate forced climate change from natural variability (Delworth et al., 2015; Deser et al., 2013; Jia et al., 2016; Kay et al., 2014; Murakami et al., 2015; Zhang, Vecchi, Murakami, Delworth, et al., 2016). Large-ensemble simulations using the same model and the same forcing provide an opportunity to assess the impacts of internal climate variability and forced climate change on the climate system (Deser et al., 2013; Kay et al., 2014). Here we use numerical simulations to assess the roles of the PDO, Atlantic warming, and anthropogenic forcing in the observed decadal change in WNP TC frequency since 1980. We use various suites of experiments (e.g., SST-nudging experiments, large-ensemble experiments (Kay et al., 2014; Zhang, Vecchi, Murakami, Delworth, et al., 2016), and perturbation experiments) with the TC-permitting Geophysical Fluid Dynamics Laboratory Forecast-oriented Low-ocean Resolution (GFDL FLOR) coupled climate model (Vecchi et al., 2014) and compare those to observations.

2. Method

2.1. TC Detection Method and Observed Data

We use a tracking algorithm (Harris et al., 2016; Zhang, Vecchi, Murakami, Villarini, & Jia, 2016) to obtain TC information from 6-hourly output from the GFDL FLOR simulations. The atmosphere and land components of FLOR (Vecchi et al., 2014) have a spatial resolution of 50 km × 50 km, while the ocean and sea ice components have a grid spacing of 1° (with a 0.333° in the deep tropics). The TC tracking algorithm uses key variables such as temperature, sea level pressure (SLP), and 10 m wind fields. As part of the TC detection algorithm, storms must maintain both a warm core and wind speeds of at least 15.75 m s^{-1} for at least 36 consecutive hours. It is noted that the threshold of wind speed might affect the number of weak TCs when tracking these storms (Daloz et al., 2015).

Observed TC data are obtained from the International Best Track Archive for Climate Stewardship (IBTrACS) including the Joint Typhoon Warning Center (JTWC), Japan Meteorological Agency (JMA), and Shanghai Typhoon Institute (STI) best track data, which have TC latitude, longitude, maximum sustained wind, minimum SLP, and date information (Knapp et al., 2010). Due to the uncertainty in tropical depression, we focus on TCs with intensity level of tropical storm or above (intensity $\geq$17.2 m/s).

For the observed environmental large-scale factors (e.g., zonal and meridional wind), we use ERA-Interim during 1979–2014 (Dee et al., 2011). The observed SST is based on the Hadley Center Global Sea Ice and Sea Surface Temperature data set (HadISST1, Rayner et al., 2003).

2.2. Large-Ensemble Multidecadal Simulations

We have two sets of large-ensemble multidecadal simulations for the period of 1941–2050 using GFDL FLOR with flux adjustments (Delworth et al., 2015; Murakami et al., 2015; Yang et al., 2015; Zhang, Vecchi, Murakami, Delworth, et al., 2016). For the 35-member all_forcing experiments, historical anthropogenic forcing and aerosols are prescribed for 1941–2005, and future levels are prescribed under Representative Concentration Pathways (RCP) 4.5 scenarios for 2006–2050. We also have 30-member "natural_forcing (or 1941 forcing)" experiments that use the same experimental settings as "all_forcing" except that anthropogenic forcing and aerosols are prescribed using the 1941 levels. It is noted that these multidecadal simulations (i.e., all_forcing and natural_forcing) are not initialized experiments. We also run 35-member experiments with the observed wind stress intensified since 1979 under "all_forcing" (denoted as all_forcing_stress, see Delworth et al., 2015 for details).

2.3. SST- and SSS-Nudging Experiments

We have the SST-restoring/nudging and sea surface salinity (SSS)-restoring/nudging experiments with FLOR at 5 day and 10 day restoring time scales (Vecchi et al., 2014). The SST-restoring experiments are defined as follows. The restoring of SST in the model to the observed estimates is represented by

$$\frac{dT}{dt} = \xi + \frac{T(\text{obs}) - T(\text{model})}{\tau} \quad (1)$$

where ξ is the SST tendency in the coupled climate model, τ is the constant restoring time scale (e.g., 5 day or

10 day), dT represents the change of SST and dt change of time. T(obs) represents a space- and time-dependent array of the observed estimates of SST, whereas T(model) is the SST simulated by the model. The larger the τ, the more relaxed the coupling and the weaker the nudging/restoring of SST. The experiments performed in this manner are different from Atmospheric Model Intercomparison Project (AMIP) experiments because the simulated SST is allowed to change during the integration. Therefore, these experiments are designed to evaluate the impacts of SST variability (e.g., observed estimates of SST and climate modes) and to partially allow air-sea interactions. Recently, Scoccimarro et al. (2017) found that the high-frequency (subdaily) coupling is essential to reduce biases in TC activity compared with AMIP simulations and with low-frequency (daily) coupled simulations. Therefore, the restoring experiment might lead to an overestimation of TC count due to its limitation in fully representing atmosphere-ocean feedbacks.

2.4. Control and Perturbation Experiments

We run a suite of perturbation experiments to assess the responses of the climate system to anomalous SST patterns associated with the AMO and PDO. We ran three experiments: the control experiment (CLIMO) and two perturbation experiments. A reference climatological experiment (CLIMO) is prepared by nudging the SST to the repeating annual cycle of global climatological SST from the long-term control experiment of FLOR; the perturbation experiment (PAMO) is designed by prescribing the annual cycle of climatological SST outside the AMO region and the overlapping of the annual cycle of climatological SST and SST anomalies associated with the positive AMO mode inside the AMO region (0–60°N, 60°W–0) at 5 day restoring time scale (Figure S1 in the supporting information). The AMO domain here is similar to the domain used in Trenberth and Shea (2006). The subtraction of the control experiment from the perturbation experiment (PAMO minus CLIMO) produces the net influence of PAMO. The perturbation experiment "NPDO" is designed by prescribing the annual cycle of climatological SST outside the tropical Pacific region and the overlapping of the annual cycle of climatological SST and SST anomalies associated with NPDO inside the tropical Pacific (30°S–30°N, 130°E–70°W). The subtraction of the control experiment from the perturbation experiment (NPDO minus CLIMO) produces the net influence of NPDO. Both CLIMO, PAMO, and NPDO experiments are spun up for 100 years and are further integrated for 60 years.

3. Results

3.1. Decadal Change in WNP TC Activity

The decadal change (defined as the difference between two periods: 1997–2014 and 1980–1996) in WNP TC frequency during June–November (JJASON) is identified using the best track data of IBTrACS (Figure 1). There is a sharp decrease in the WNP TC frequency during 1997–2014 compared to the 1980–1996 period in the best track data. The average WNP TC frequency in the period 1980–1996 is 22.4 TCs/year, while it drops sharply to 18.4 TCs/year during 1997–2014. The observed difference in the WNP TC frequency of 4.1 TCs/year between the two periods is significant at the 0.01 level based on the Student's t test (Table 1).

3.2. Decadal Change of WNP TC Activity in GFDL FLOR

We examined whether and the extent to which the GFDL FLOR climate model can reproduce the observed decadal change in WNP TC frequency. The average WNP TC frequencies in the SST- and SSS-nudging experiments (hereafter denoted as SST-nudging experiments for simplicity, with six members) of FLOR in 1980–1996 and 1997–2014 are 24.8 TCs/year and 22.1 TCs/year, showing a statistically significant decrease in WNP TC frequency in the later period (Table 1). The decreased frequencies of WNP TCs in the six-member SST-nudging experiments between 1997–2014 and 1980–1996 range from 1.2 to 3.8 TCs/year, significant at the 0.05 level. Overall, FLOR exhibits larger climatological values for the WNP TC frequency compared to the observations. Based on these results and previous studies (Zhang, Vecchi, Murakami, Delworth, et al., 2016; Zhang, Villarini, et al., 2016; Zhang, Vecchi, Villarini, Murakami, Gudgel, & Yang, 2017; Zhang, Vecchi, Villarini, Murakami, Rosati, et al., 2017), FLOR captures reasonably well the observed decadal change of WNP TC frequency in the SST-nudging experiments, suggesting that the SST change may play an important role in the decadal change of WNP TC frequency. We also assess the role of anthropogenic forcing in the decadal change of WNP TC frequency using large-ensemble experiments with FLOR, and we find relatively minor role played by anthropogenic forcing.

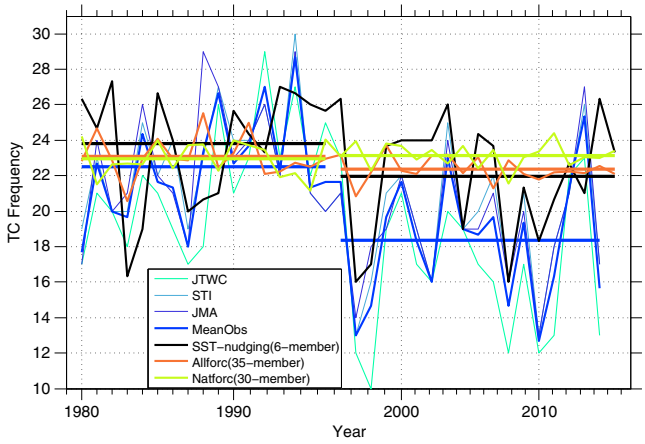

Figure 1. Observed WNP TC frequencies during peak TC season (JJASON) using JTWC (cyan), JMA (dark blue), STI (light blue) best track data and the mean frequency collected by IBTrACS (denoted by "MeanObs"), the SST-nudging experiments with FLOR (black, six-member), the large-ensemble mean WNP TC frequencies during the peak TC season in all_forcing (Allforc) experiments (brown, 35 members), and natural_forcing (Natforc) experiments (light green, 30 members) for 1980–2014 and their mean values (horizontal lines) in 1980–1996 and 1997–2014.

The WNP TC frequencies in the two periods (i.e., 1997–2014 and 1980–1996) in the large-ensemble all_forcing and natural_forcing (1941 forcing) experiments are shown in Figure 1. There is a drop (−0.7 TCs/year) in average WNP TC frequency from 23.1 TCs/year to 22.4 TCs/year in the all_forcing experiments, while there is a slight increase (0.2 TC/year) from 23.0 TCs/year to 23.2 TCs/year in the natural_forcing experiments. The decrease in WNP TC frequency in the all_forcing experiments (−0.7 TCs/year) is much smaller than that in the observations (−4.1 TCs/year). The relatively small nominal difference (−0.9 TCs/year, which is not significant) in the decadal change of WNP TC frequency between all_forcing and natural_forcing is largely due to the effects of anthropogenic forcing changes (Figure 1 and Table 1). This indicates that the anthropogenic forcing plays only a secondary role in this decadal change (Table 1).

Figure 2 shows the differences in WNP TC genesis density between 1980–1996 and 1997–2014 in the observations and simulations with FLOR. The differences in observed TC genesis density are characterized by strong negative genesis anomalies in the eastern WNP and weak positive genesis anomalies in the western WNP (Figure 2a), consistent with findings from previous studies (Lin & Chan, 2015; Liu & Chan, 2012; B. Wang & Chan, 2002; Zhang, Vecchi, Murakami, Villarini, & Jia, 2016; Zhang, Vecchi, Villarini, Murakami, Rosati, et al., 2017). The decadal change of TC genesis density in the all_forcing experiments is largely characterized by negative anomalies, albeit with a much smaller magnitude (Figure 2b). The regions with negative anomalies in TC genesis density are larger than those with positive anomalies. The six-member SST-nudging experiments largely represent the influences of observed SST on this decadal change. The observed decadal change of WNP TC genesis pattern is captured reasonably well by the SST-nudging experiments with FLOR (Figure 2c), though there are slight discrepancy in the local changes of TC genesis density. This indicates that the SST changes during 1997–2014 and 1980–1996 play a central role in the decadal change of WNP TC frequency. The SST differences between 1997–2014 and 1980–1996 are mainly characterized by negative PDO (NPDO) in the Pacific and a positive AMO (PAMO) pattern in the North Atlantic (Figure S2). Perturbation experiments are thus performed to examine the relative roles of NPDO and PAMO in the change of WNP TC frequency.

3.3. Perturbation Experiments: PAMO or NPDO

The perturbation experiments are forced by the anomalous NPDO and PAMO SST patterns, respectively (see section 2.4 and Figure S1 for details). The subtraction of the control experiment (CLIMO) from the perturbation experiment (NPDO/PAMO minus CLIMO) produces the net influence of the NPDO/PAMO modes. Previous studies reported that the NPDO phase is tied to the intensification of trades in the tropical Pacific (Delworth et al., 2015; England et al., 2014; Sun et al., 2017). We also analyze the 35-member all_forcing_stress minus all_forcing experiments to assess the impacts of the strengthened wind stress (trade winds) in the tropical Pacific on the decadal change of WNP TCs. The NPDO experiment produces 0.7 fewer TCs than the CLIMO experiment on average, failing to pass the Student's *t* test (Table S1). However, the PAMO experiment produces 4.2 fewer TCs/year than the CLIMO experiment, which is statistically significant at the 0.01 level and similar to the observed difference (i.e., 4.1 TCs/year) in WNP TC frequency between the two periods (Tables 1 and S1). The strong impact of PAMO on WNP TC frequency than NPDO is also supported by the correlation analysis between the AMO index and WNP TC frequency for the period 1980–2014 (correlation coefficient of −0.5, significant at the 0.05 level), dramatically higher than 0.16 for the PDO index which is not statistically significant (Table S2). The

Table 1
WNP TC Frequency in 1980–1996 and 1997–2014 and Their Differences Between the Observations, SST-Nudging Experiments, and the Large-Ensemble Multidecadal All_Forcing and Natural_Forcing (1941_Forcing) Experiments With FLOR

	TCF		
	1997–2014	1980–1996	Diff
JMA	19.1	22.9	−3.8*
JTWC	19.2	22.9	−3.7*
STI	16.8	21.7	−4.9*
MeanObs	18.4	22.5	−4.1*
SST-Nudging Exp	22.1	24.8	−2.7*
All_forcing Exp	22.4	23.1	−0.7*
Natural_forcing Exp	23.2	23.0	0.2

*The difference is significant at the 0.05 level based on Student's *t* test.

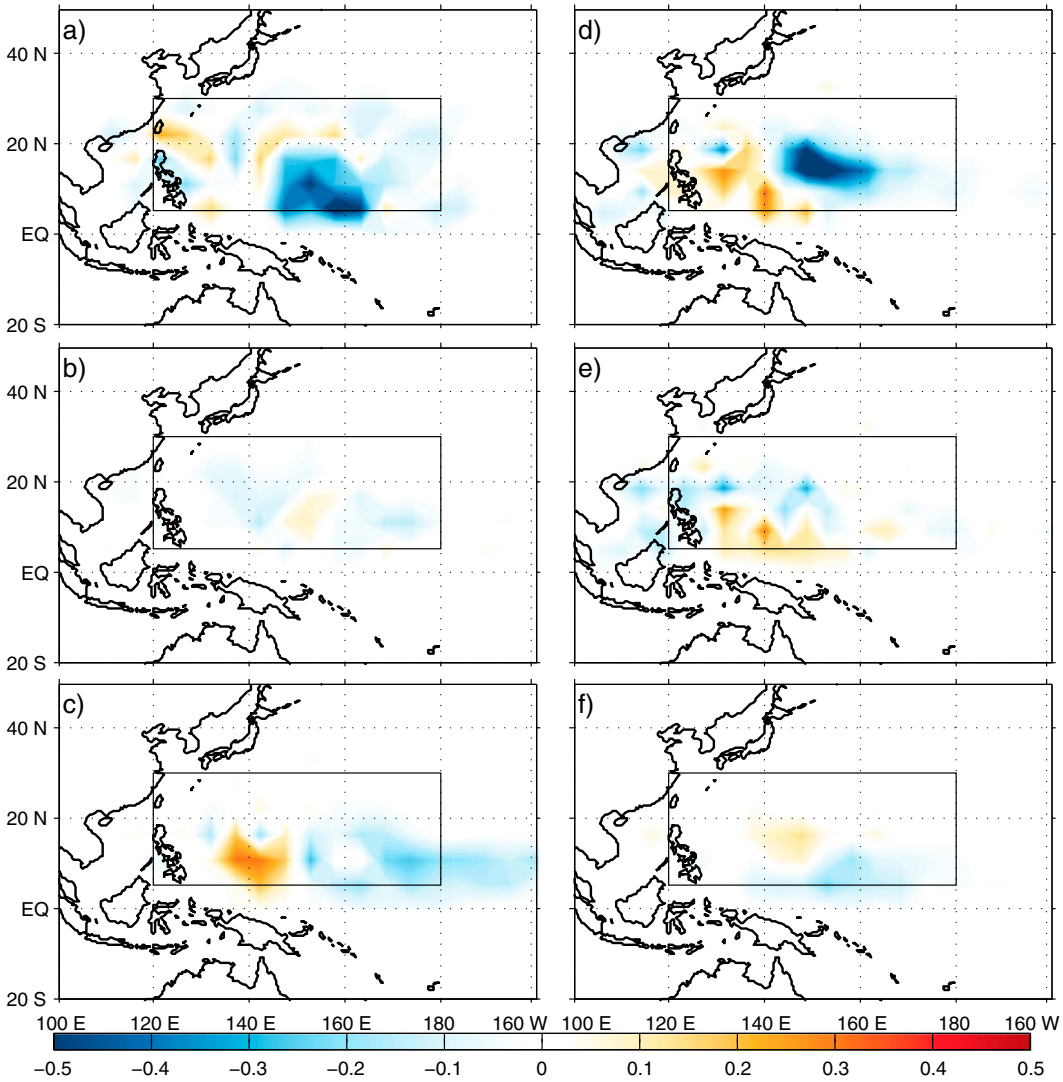

Figure 2. TC genesis density differences (shading, 5° × 5°) in 1997–2014 minus 1980–1996 in (a) the observations (averaged over JMA, JTWC, and STI best track data), (b) large-ensemble all_forcing minus natural_forcing experiments, and (c) the SST-nudging experiments with FLOR, and the anomalies of TC genesis in (d) PAMO minus CLIMO, (e) NPDO minus CLIMO, and (f) all_forcing_stress minus all_forcing experiments (1997–2014) with FLOR. The all_forcing_stress minus all_forcing experiments indicate the responses of the TC genesis density to the strengthened wind stress in the tropics since 1997. The rectangle shows the main develop region (MDR) in the WNP.

perturbation experiments indicate that the PAMO pattern strongly suppresses WNP TC activity and that the PAMO plays a leading role in the observed decadal change in WNP TC activity since 1980. The NPDO plays a much weaker role in modulating the WNP TC frequency than the PAMO pattern (Figures 2d and 2e). The anomalies in TC genesis density in PAMO minus CLIMO are similar to those in the observations (1997–2014 minus 1980–1996), while those in NPDO minus CLIMO are much weaker than in the observations. We would expect similar results if we examine the impacts of NPDO and PAMO on TC days instead of TC frequency because the observed suppressed TC geneses in the eastern portion of WNP are reasonably reproduced in the PAMO experiment. Suppressed TC geneses in the eastern portion of WNP indicate less TCs with longer lifespan, which is a good indicator of TC days.

To further substantiate these findings, we also analyze the differences in WNP TC frequency between all_forcing_stress and all_forcing experiments for the period 1997–2014. The TC genesis density anomalies in all_forcing_stress minus all_forcing are very small (Figure 2f), indicating that the intensified wind stress plays a marginal role in the decadal change of WNP TC genesis. The FLOR experiments forced with the observed strengthened wind stress produce the same average TC frequency (19.2 TCs/year) as those

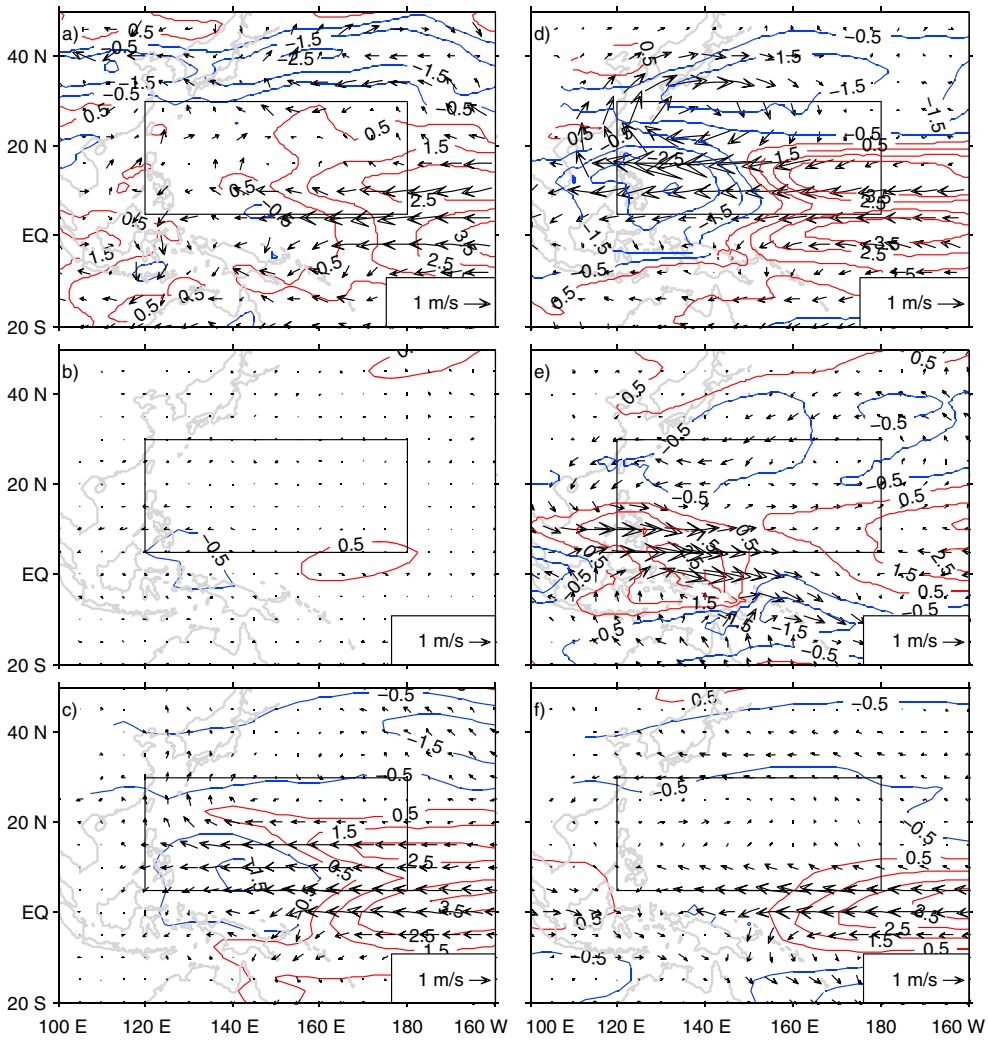

Figure 3. Vertical wind shear (contour, unit: m s^{-1}) and 850 hPa wind fields (vector, unit: m s^{-1}) differences in 1997–2014 minus 1980–1996 in (a) the observations, (b) large-ensemble multidecadal all_forcing minus natural_forcing (Allforc minus Natforc) experiments, and (c) the SST-nudging experiments with FLOR, and the anomalies of vertical wind shear and 850 hPa wind fields in (d) PAMO minus CLIMO, (e) NPDO minus CLIMO, and (f) all_forcing_stress minus all_forcing experiments (1997–2014) with FLOR. The rectangle shows the MDR in the WNP.

without it, further indicating a minor role played by the intensified trade winds after 1997 in the decadal change of WNP TC activity.

3.4. Physical Mechanisms

Previous studies highlighted the role of vertical wind shear (i.e., wind differences between 850 hPa and 200 hPa levels) and 850 hPa wind flow pattern (cyclonic/anticyclonic) in modulating WNP TC genesis frequency (Lin & Chan, 2015; Liu & Chan, 2012; Wang & Chan, 2002; Zhang, Vecchi, Murakami, Villarini, & Jia, 2016; Zhang, Vecchi, Villarini, Murakami, Rosati, et al., 2017). Here we assess the differences in vertical wind shear and 850 hPa wind fields between 1980–1996 and 1997–2014.

The decadal change in vertical wind shear is consistent with TC genesis density in the observations (Figures 2a and 3a). In other words, there are strong positive vertical wind shear anomalies in the eastern WNP (Figure 3a), responsible for the suppressed TC genesis there (Figure 2a). The 850 hPa wind difference is largely characterized by an anticyclonic flow pattern in the WNP, which acts to suppress TC genesis (Figure 3a). In the western part of the WNP, there are small regions with negative vertical wind shear anomalies and a cyclonic flow pattern (Figure 3a), responsible for some positive TC genesis anomalies in the WNP in the observations (Figure 2a). The positive anomalies in vertical wind shear in the eastern part of the WNP are

also present in the large-ensemble all_forcing minus natural_forcing (i.e., anthropogenic forcing) experiments, with a much smaller magnitude in the experiments compared with the observations (Figure 3b). The vertical wind shear differences are consistent with the differences in genesis density in all_forcing minus natural_forcing experiments (Figures 2b and 3b). It also suggests that a small magnitude in the VWS differences is responsible for a smaller difference in WNP TC frequency in all_forcing minus natural_forcing experiments. In addition, the large-scale circulation differences represented by the 850 hPa wind flow (anticyclonic flow) in the all_forcing minus natural_forcing experiments are much weaker than in the observations (Figures 3a and 3b). On the other hand, the vertical wind shear differences in the SST-nudging experiments bear strong resemblance with the observations, with strong positive anomalies in the eastern WNP and negative anomalies in the southwestern WNP (Figure 3c). Such patterns in vertical wind shear are consistent with TC genesis differences in the SST-nudging experiments (Figures 2c and 3c). The observed precipitation differences in the two periods are also well reproduced in the SST-nudging experiments, while the all_forcing minus natural_forcing experiments fail to reproduce these differences (Figure S3). Therefore, these results provide further evidence of the dominant impacts of vertical wind shear on WNP TC genesis in model simulations and observations.

We also analyzed the vertical wind shear and 850 hPa level wind fields from the perturbation experiments in order to assess the changes in TC genesis and frequency. The vertical wind shear differences in PAMO minus CLIMO experiments are characterized by strong positive (negative) anomalies in the eastern (western) part of the WNP (Figure 3d). The magnitude of such anomalies in the eastern part of the WNP is similar to the observations. The SST warming anomalies in the North Atlantic (PAMO) tend to strongly suppress TC genesis in the eastern WNP by altering the Walker circulation to intensify vertical wind shear.

The 850 hPa wind fields in PAMO minus CLIMO produce a strong anticyclonic flow in the WNP, similar to the anticyclonic flow in the observations (Figures 2d and 3d). However, the anticyclonic flow in PAMO minus CLIMO (Figure 3d) is stronger than that in the observed differences in 850 hPa wind fields between 1980–1996 and 1997–2014 (Figure 3d). The strong anticyclonic flow pattern may be associated with suppressed convection in the WNP represented by negative precipitation anomalies (Figure S4). The vertical wind shear anomalies in PAMO minus CLIMO (Figures 3d) are consistent with the anomalies in TC genesis density (Figure 2d). The vertical wind shear anomalies in NPDO minus CLIMO are also characterized by positive anomalies in the western WNP. However, the magnitude of vertical wind shear in NPDO minus CLIMO is much smaller than those in PAMO and the observations (Figures 3d and 3e). Moreover, the large-scale circulation in the WNP in NPDO minus CLIMO experiments has a characteristic cyclonic flow pattern in the WNP, different from the observations and the SST-nudging experiments. The characteristic cyclonic flow in NPDO minus CLIMO may be forced by the SST-related heating represented by the positive precipitation anomalies in the tropical western Pacific (Figure S4), similar to classic Matsuno-Gill responses (Gill, 1980) (Figure 3e). Although NPDO suppresses TC genesis in the western WNP (Figure 2e), the magnitude of this suppression of TC genesis is smaller than that of the PAMO (Figure 2d). In the western WNP, the cyclonic flow pattern and negative vertical wind shear anomalies associated with Matsuno-Gill responses enhance TC genesis in the NPDO minus CLIMO experiments (Figure 3e). The vertical wind shear anomalies in all_forcing_stress minus all_forcing experiments are quite weak in the WNP (Figure 3f). The anomalous 850 hPa wind fields in all_forcing_stress minus all_forcing is also quite weak compared with PAMO and NPDO experiments (Figures 3d–3f).

The observed differences in the vertical profile of zonal wind and vertical velocity between 1997–2014 and 1980–1996 feature anomalous upper level westerlies and lower-level easterlies in the eastern part of the WNP (Figure S5a). Given the climatological westerlies and easterlies in the upper and lower levels, the intensified upper-level westerlies and low-level easterlies in observations (Figure S5a) induces stronger vertical wind shear (Figure 3a), which suppresses TC genesis in the eastern WNP. In addition, the observed lower level and upper wind changes in the eastern WNP are reasonably captured by the PAMO experiment, though the upper level wind anomalies in the PAMO experiment (Figure S5b) is larger than the observed ones (Figure S5a). The converse is true for the western WNP, where there is enhanced TC genesis in the PAMO experiment (Figure 2d) accompanied by reduced vertical wind shear (Figure 3d). The excessive vertical wind shear in the PAMO experiment suggests that some other factors may play some role in the vertical wind shear during this period, which needs further investigation. However, the wind upper and lower level wind

anomalies in the NPDO experiment (NPDO minus CLIMO) are markedly weaker than the observations and the PAMO experiment, in agreement with weak vertical wind shear anomalies (Figure S5c). Therefore, the vertical wind shear and 850 hPa wind fields in the perturbation experiments support the anomalies in WNP TC genesis/frequency.

4. Conclusions and Discussion

We have assessed the roles of NPDO, PAMO, and anthropogenic forcing in the decadal change in WNP TC frequency using observations and a set of high-resolution climate model (GFDL-FLOR) experiments. The decadal change of WNP TC frequency between 1980–1996 and 1997–2014 in the observations is largely reproduced by the SST-nudging experiments with FLOR. The recent decadal change of WNP TC frequency was primarily driven by the intensified vertical wind shear in the southeastern WNP induced by the SST warming in the North Atlantic (i.e., PAMO), with the SST anomalies associated with NPDO playing a secondary role. Overall, FLOR reproduces reasonably well the observed vertical wind shear anomalies (1997–2014 minus 1980–1996) in the PAMO experiment, although the vertical wind shear anomalies in FLOR are slightly stronger than observations with some discrepancy in the spatial patterns of vertical wind shear anomalies, probably associated with model biases and other factors that modulate WNP TCs. For example, WNP TC frequency can also be influenced by factors from high-latitude regions (Ho et al., 2005; Wang et al., 2007), which are not considered in this study. Given the key role of the AMO in the decadal change of WNP TC activity, improving predictions and projections of WNP TC activity should include a focus on the North Atlantic and the AMO. If AMO changes the sign in the near future, we may see more typhoons in the WNP.

Acknowledgments
We are grateful to two anonymous reviewers for insightful comments. The authors acknowledge Kun Gao and Lakshmi Krishnamurthy for their helpful comments on an earlier version of this manuscript. This material is based in part upon work supported by the National Science Foundation under grants AGS-1262091 and AGS-1262099. The TC data are obtained from https://www.ncdc.noaa.gov/ibtracs/. Data for environmental variables (e.g., wind fields) are obtained from ERA-Interim (https://www.ecmwf.int/en/forecasts/datasets/reanalysis-datasets/era-interim). The climate experiments are performed with GFDL FLOR (available from https://www.gfdl.noaa.gov/cm2-5-and-flor/). The SST data are obtained from https://www.metoffice.gov.uk/hadobs/hadisst/. The code for processing data is available upon request.

References

Chan, J. C. L. (2008). Decadal variations of intense typhoon occurrence in the western North Pacific. *Proceedings of the Royal Society A: Mathematical, Physical and Engineering Science*, *464*(2089), 249–272.

Choi, Y., Ha, K.-J., Ho, C.-H., & Chung, C. (2015). Interdecadal change in typhoon genesis condition over the western North Pacific. *Climate Dynamics*, *45*(11-12), 3243–3255. https://doi.org/10.1007/s00382-015-2536-y

Daloz, A. S., Camargo, S. J., Kossin, J. P., Emanuel, K., Horn, M., Jonas, J. A., … Zhao, M. (2015). Cluster analysis of downscaled and explicitly simulated North Atlantic tropical cyclone tracks. *Journal of Climate*, *28*(4), 1333–1361. https://doi.org/10.1175/jcli-d-13-00646.1

Dee, D. P., Uppala, S. M., Simmons, A. J., Berrisford, P., Poli, P., Kobayashi, S., … Vitart, F. (2011). The ERA-Interim reanalysis: Configuration and performance of the data assimilation system. *Quarterly Journal of the Royal Meteorological Society*, *137*(656), 553–597. https://doi.org/10.1002/qj.828

Delworth, T. L., Zeng, F., Rosati, A., Vecchi, G. A., & Wittenberg, A. T. (2015). A link between the hiatus in global warming and North American drought. *Journal of Climate*, *28*(9), 3834–3845. https://doi.org/10.1175/JCLI-D-14-00616.1

Delworth, T. L., Zeng, F., Vecchi, G. A., Yang, X., Zhang, L., & Zhang, R. (2016). The North Atlantic oscillation as a driver of rapid climate change in the Northern Hemisphere. *Nature Geoscience*, *9*(7), 509–512. https://doi.org/10.1038/ngeo2738

Deser, C., Phillips, A. S., Alexander, M. A., & Smoliak, B. V. (2013). Projecting North American climate over the next 50 years: Uncertainty due to internal variability*. *Journal of Climate*, *27*(6), 2271–2296. https://doi.org/10.1175/JCLI-D-13-00451.1

Emanuel, K. (2005a). *Divine Wind-The History and Science of Hurricanes* (pp. 1–22). New York: Oxford University Press.

Emanuel, K. (2005b). Increasing destructiveness of tropical cyclones over the past 30 years. *Nature*, *436*(7051), 686–688. https://doi.org/10.1038/nature03906

Emanuel, K. (2007). Environmental factors affecting tropical cyclone power dissipation. *Journal of Climate*, *20*(22), 5497–5509. https://doi.org/10.1175/2007JCLI1571.1

England, M. H., McGregor, S., Spence, P., Meehl, G. A., Timmermann, A., Cai, W., … Santoso, A. (2014). Recent intensification of wind-driven circulation in the Pacific and the ongoing warming hiatus. *Nature Climate Change*, *4*(3), 222–227. https://doi.org/10.1038/nclimate2106

Gill, A. E. (1980). Some simple solutions for heat-induced tropical circulation. *Quarterly Journal of the Royal Meteorological Society*, *106*(449), 447–462. https://doi.org/10.1002/qj.49710644905

Harris, L. M., Lin, S.-J., & Tu, C. (2016). High-resolution climate simulations using GFDL HiRAM with a stretched global grid. *Journal of Climate*, *29*(11), 4293–4314. https://doi.org/10.1175/jcli-d-15-0389.1

He, H., Yang, J., Gong, D., Mao, R., Wang, Y., & Gao, M. (2015). Decadal changes in tropical cyclone activity over the western North Pacific in the late 1990s. *Climate Dynamics*, *45*(11-12), 3317–3329. https://doi.org/10.1007/s00382-015-2541-1

Ho, C.-H., Kim, J.-H., Kim, H.-S., Sui, C.-H., & Gong, D.-Y. (2005). Possible influence of the Antarctic Oscillation on tropical cyclone activity in the western North Pacific. *Journal of Geophysical Research*, *110*, D19104. https://doi.org/10.1029/2005JD005766

Jia, L., Vecchi, G. A., Yang, X., Gudgel, R. G., Delworth, T. L., Stern, W. F., … Zeng, F. (2016). The roles of radiative forcing, sea surface temperatures, and atmospheric and land initial conditions in US summer warming episodes. *Journal of Climate*, *29*(11), 4121–4135. https://doi.org/10.1175/JCLI-D-15-0471.1

Kay, J. E., Deser, C., Phillips, A., Mai, A., Hannay, C., Strand, G., … Vertenstein, M. (2014). The Community Earth System Model (CESM) large ensemble project: A community resource for studying climate change in the presence of internal climate variability. *Bulletin of the American Meteorological Society*, *96*(8), 1333–1349. https://doi.org/10.1175/BAMS-D-13-00255.1

Knapp, K. R., Kruk, M. C., Levinson, D. H., Diamond, H. J., & Neumann, C. J. (2010). The International Best Track Archive for Climate Stewardship (IBTrACS). *Bulletin of the American Meteorological Society*, *91*(3), 363–376. https://doi.org/10.1175/2009BAMS2755.1

Knutson, T., McBride, J., Chan, J., Emanuel, K., Holland, G., Landsea, C., … Sugi, M. (2010). Tropical cyclones and climate change. *Nature Geoscience*, *3*(3), 157–163. https://doi.org/10.1038/ngeo779

Kossin, J. P., Emanuel, K. A., & Camargo, S. J. (2016). Past and projected changes in western North Pacific tropical cyclone exposure. *Journal of Climate*, *29*(16), 5725–5739. https://doi.org/10.1175/jcli-d-16-0076.1

Kucharski, F., Ikram, F., Molteni, F., Farneti, R., Kang, I.-S., No, H.-H., … Mogensen, K. (2016). Atlantic forcing of Pacific decadal variability. *Climate Dynamics*, *46*(7-8), 2337–2351. https://doi.org/10.1007/s00382-015-2705-z

Li, X., Xie, S.-P., Gille, S. T., & Yoo, C. (2015). Atlantic-induced pan-tropical climate change over the past three decades. *Nature Climate Change*, *6*(3), 275–279. https://doi.org/10.1038/nclimate2840

Lin, I. I., & Chan, J. C. L. (2015). Recent decrease in typhoon destructive potential and global warming implications. *Nature Communications*, *6*, 7182. https://doi.org/10.1038/ncomms8182

Liu, K. S., & Chan, J. C. L. (2012). Inactive period of western North Pacific tropical cyclone activity in 1998–2011. *Journal of Climate*, *26*(8), 2614–2630. https://doi.org/10.1175/JCLI-D-12-00053.1

Mantua, N. J., Hare, S. R., Zhang, Y., Wallace, J. M., & Francis, R. C. (1997). A Pacific Interdecadal Climate Oscillation with impacts on Salmon production. *Bulletin of the American Meteorological Society*, *78*(6), 1069–1079. https://doi.org/10.1175/1520-0477(1997)078%3C1069:apicow%3E2.0.co;2

McGregor, S., Timmermann, A., Stuecker, M. F., England, M. H., Merrifield, M., Jin, F.-F., & Chikamoto, Y. (2014). Recent Walker circulation strengthening and Pacific cooling amplified by Atlantic warming. *Nature Climate Change*, *4*(10), 888–892. https://doi.org/10.1038/nclimate2330

Murakami, H., Vecchi, G. A., Delworth, T. L., Paffendorf, K., Jia, L., Gudgel, R., & Zeng, F. (2015). Investigating the influence of anthropogenic forcing and natural variability on the 2014 Hawaiian hurricane season. *Bulletin of the American Meteorological Society*, *96*(12), S115–S119. https://doi.org/10.1175/BAMS-D-15-00119.1

Murakami, H., Wang, Y., Yoshimura, H., Mizuta, R., Sugi, M., Shindo, E., … Kusunoki, S. (2012). Future changes in tropical cyclone activity projected by the new high-resolution MRI-AGCM. *Journal of Climate*, *25*(9), 3237–3260. https://doi.org/10.1175/JCLI-D-11-00415.1

Peduzzi, P., Chatenoux, B., Dao, H., De Bono, A., Herold, C., Kossin, J., … Nordbeck, O. (2012). Global trends in tropical cyclone risk. *Nature Climate Change*, *2*(4), 289–294. https://doi.org/10.1038/nclimate1410

Rayner, N., Parker, D., Horton, E., Folland, C., Alexander, L., Rowell, D., … Kaplan, A. (2003). Global analyses of sea surface temperature, sea ice, and night marine air temperature since the late nineteenth century. *Journal of Geophysical Research*, *108*(D14), 4407. https://doi.org/10.1029/2002JD002670

Ruprich-Robert, Y., Msadek, R., Castruccio, F., Yeager, S., Delworth, T., & Danabasoglu, G. (2017). Assessing the climate impacts of the observed Atlantic multidecadal variability using the GFDL CM2.1 and NCAR CESM1 global coupled models. *Journal of Climate*, *30*(8), 2785–2810. https://doi.org/10.1175/jcli-d-16-0127.1

Scoccimarro, E., Fogli, P. G., Reed, K. A., Gualdi, S., Masina, S., & Navarra, A. (2017). Tropical cyclone interaction with the ocean: The role of high frequency (sub-daily) coupled processes. *Journal of Climate*, *30*(1), 145–162. https://doi.org/10.1175/JCLI-D-16-0292.1

Sun, C., Kucharski, F., Li, J., Jin, F.-F., Kang, I.-S., & Ding, R. (2017). Western tropical Pacific multidecadal variability forced by the Atlantic multidecadal oscillation. *Nature Communications*, *8*, 15998. https://doi.org/10.1038/ncomms15998

Takahashi, C., Watanabe, M., & Mori, M. (2017). Significant aerosol influence on the recent decadal decrease in tropical cyclone activity over the western North Pacific. *Geophysical Research Letters*, *44*, 9496–9504. https://doi.org/10.1002/2017GL075369

Trenberth, K. E., & Shea, D. J. (2006). Atlantic hurricanes and natural variability in 2005. *Geophysical Research Letters*, *33*, L12704. https://doi.org/10.1029/2006GL026894

Vecchi, G. A., Delworth, T., Gudgel, R., Kapnick, S., Rosati, A., Wittenberg, A. T., … Zhang, S. (2014). On the seasonal forecasting of regional tropical cyclone activity. *Journal of Climate*, *27*(21), 7994–8016. https://doi.org/10.1175/JCLI-D-14-00158.1

Villarini, G., Vecchi, G. A., Knutson, T. R., Zhao, M., & Smith, J. A. (2011). North Atlantic tropical storm frequency response to anthropogenic forcing: Projections and sources of uncertainty. *Journal of Climate*, *24*(13), 3224–3238. https://doi.org/10.1175/2011jcli3853.1

Wang, B., & Chan, J. C. L. (2002). How strong ENSO events affect tropical storm activity over the western North Pacific. *Journal of Climate*, *15*(13), 1643–1658. https://doi.org/10.1175/1520-0442(2002)015%3C1643:HSEEAT%3E2.0.CO;2

Wang, H., Sun, J., & Fan, K. (2007). Relationships between the North Pacific Oscillation and the typhoon/hurricane frequencies. *Science in China Series D: Earth Sciences*, *50*(9), 1409–1416. https://doi.org/10.1007/s11430-007-0097-6

Wu, L., Wang, C., & Wang, B. (2015). Westward shift of western North Pacific tropical cyclogenesis. *Geophysical Research Letters*, *42*, 1537–1542. https://doi.org/10.1002/2015GL063450

Yang, X., Vecchi, G. A., Delworth, T. L., Paffendorf, K., Jia, L., Gudgel, R., … Underwood, S. D. (2015). Extreme North America winter storm season of 2013/14: Roles of radiative forcing and the global warming hiatus. *Bulletin of the American Meteorological Society*, *96*(12), S25–S28. https://doi.org/10.1175/BAMS-EEE_2014_ch6.1

Yu, J., Li, T., Tan, Z., & Zhu, Z. (2015). Effects of tropical North Atlantic SST on tropical cyclone genesis in the western North Pacific. *Climate Dynamics*, *46*(3-4), 865–877. https://doi.org/10.1007/s00382-015-2618-x

Zhang, R., & Delworth, T. L. (2007). Impact of the Atlantic Multidecadal Oscillation on North Pacific climate variability. *Geophysical Research Letters*, *34*, L23708. https://doi.org/10.1029/2007GL031601

Zhang, W., Vecchi, G. A., Murakami, H., Delworth, T. L., Paffendorf, K., Jia, L., … Yang, X. (2016). Influences of natural variability and anthropogenic forcing on the extreme 2015 accumulated cyclone energy in the western North Pacific. *Bulletin of the American Meteorological Society*, *97*(12), S131–S135. https://doi.org/10.1175/bams-d-16-0146.1

Zhang, W., Vecchi, G. A., Murakami, H., Villarini, G., & Jia, L. (2016). The Pacific meridional mode and the occurrence of tropical cyclones in the western North Pacific. *Journal of Climate*, *29*(1), 381–398. https://doi.org/10.1175/jcli-d-15-0282.1

Zhang, W., Vecchi, G. A., Villarini, G., Murakami, H., Gudgel, R., & Yang, X. (2017). Statistical–dynamical seasonal forecast of western North Pacific and East Asia landfalling tropical cyclones using the GFDL FLOR coupled climate model. *Journal of Climate*, *30*(6), 2209–2232. https://doi.org/10.1175/jcli-d-16-0487.1

Zhang, W., Vecchi, G. A., Villarini, G., Murakami, H., Rosati, A., Yang, X., … Zeng, F. (2017). Modulation of western North Pacific tropical cyclone activity by the Atlantic Meridional Mode. *Climate Dynamics*, *48*(1-2), 631–647. https://doi.org/10.1007/s00382-016-3099-2

Zhang, W., Villarini, G., Vecchi, G. A., Murakami, H., & Gudgel, R. (2016). Statistical-dynamical seasonal forecast of western North Pacific and East Asia landfalling tropical cyclones using the high-resolution GFDL FLOR coupled model. *Journal of Advances in Modeling Earth Systems*, *8*(2), 538–565. https://doi.org/10.1002/2015MS000607